Berna, T. J., M. H. Locke, and A. W. Westerberg, "A New Approach to Optimization of Chemical Processes," *AIChE J.*, **26**, 1 (1980).
Biegler, L. T., and R. R. Hughes, "Approximation Programming of Chemical Processes with Q/LAP," *Chem. Eng. Prog.*, (April, 1981).
Black, C., R. A. Golding, and D. E. Ditsler, "Azeotropic Distillation Results from Automatic Computer Calculations," *Extractive and Azeotropic Distillation*, Advances in Chemistry Series 115, ACS (1972).
Boston, J. F., "Algorithms for Distillation Calculations with Bounded-Variable Design Constraints and Equality- or Inequality-Constrained Optimization," Energy Laboratory, M.I.T., Cambridge, MA (1978).
Gmehling, J., and U. Onken, *Vapor-Liquid Equilibrium Data Collection*, DECHEMA, Chemistry Data Series, I, Part 1, Verlag & Druckerei Friedrick Bischoff, Frankfurt (1977).
Jirapongphan, S., *Simultaneous Modular Convergence Concept in Process Flowsheet Optimization*, D.Sc Dissertation, M.I.T. (1980).
Jirapongphan, S., J. F. Boston, H. I. Britt, and L. B. Evans, "A Nonlinear Simultaneous Modular Algorithm for Process Flowsheet Optimization," Dept. of Chem. Eng. and Energy Lab., M.I.T., Cambridge, MA (1980).
Magnussen, T., M. L. Michelsen, and A. Fredenslund, "Azeotropic Distillation Using UNIFAC," *Inst. Chem. Eng. Symp. Ser. No. 56*, Third Int'l Symp. on Distillation, ICE, Rugby, Warwickshire, England (1979).
Napthali, L. M., and D. P. Sandholm, "Multicomponent Separation Calculations by Linearization," *AIChE J.*, **17**, 1 (1971).
Norman, W. S., "The Dehydration of Ethanol by Azeotropic Distillation, Vapour-Liquid Equilibrium Data for the System Ethanol-Benzene-Water," *Trans. Inst. Chem. Eng.*, **23**, 66 (1945).
Powell, M. J. D., "A Fast Algorithm for Nonlinearly Constrained Optimization Calculations," presented at 1977 Dundee Conference on Numerical Analysis (1977).
Prausnitz, J. M., T. F. Anderson, E. A. Grens, C. A. Eckert, R. Hsieh, and J. P. O'Connell, *Computer Calculations for Multicomponent Vapor-Liquid and Liquid-Liquid Equilibria*, Prentice-Hall (1980).
Prokopakis, G. J., and W. D. Seider, "Dynamic Simulation of Distillation Towers," presented at the 73rd Annual Meeting of AIChE, Chicago (1980).
Prokopakis, G. J., B. A. Ross, and W. D. Seider, "Azeotropic Distillation Towers with Two Liquid Phases," *Foundations of Computer-aided Chemical Process Design*, eds., R. S. H. Mah and W. D. Seider, AIChE (1981).
Reid, R. C., J. M. Prausnitz, and T. K. Sherwood, *Properties of Gases and Liquids*, Third Edition, McGraw-Hill (1977).
Robinson, C. S., and E. R. Gilliland, *Elements of Fractional Distillation*, McGraw-Hill, p. 312 (1950).
Ross, B. A., and W. D. Seider, "Simulation of Three-Phase Distillation Towers," *Comp. and Chem. Eng.*, **5**, 1 (1981).
Van Dongen, D. B., and M. F. Doherty, "Restrictions on the Behavior of Multicomponent Azeotropic Distillation Processes," Paper No. 66C, 72nd Annual Meeting of AIChE, San Francisco, CA (1979).

Manuscript received August 4, 1981; revision received January 26, and accepted February 22, 1982.

Absorption of Sulfur Dioxide into Aqueous Double Slurries Containing Limestone and Magnesium Hydroxide

The absorption of dilute SO_2 into aqueous double slurries containing $CaCO_3$ and $Mg(OH)_2$ was carried out using a stirred tank with a plane gas-liquid interface. The absorption rate increased and finally reached that under the completely gas-film controlled conditions as the absorption process proceeded. The desulfurization process using the double slurry was formulated by a two-reaction-plane model in which there are no particles suspended in-between the interface and the primary reaction plane. It was suggested from comparison of the experimental absorption rates with the theoretical predictions that 40 to 60% of the absorbed sulfur dioxide may be present as an effective magnesium sulfite ion pair.

E. SADA, H. KUMAZAWA
and
H. NISHIMURA

Department of Chemical Engineering
Kyoto University
Kyoto, Japan

SCOPE

The elementary processes involved in chemical absorption into a slurry are: (i) diffusion of solute gas in the gas film, (ii) diffusion in the liquid film, (iii) chemical reaction, and (iv) dissolution of solids (one of the reactants). Elementary process (ii) combined with (iii) is called chemical absorption or gas absorption accompanied by chemical reaction. The chemical absorption and the solid dissolution are transfer processes in parallel or in series, depending upon whether the suspended particle size is much smaller than or is comparable to the thickness of the liquid film. When this transfer process is assumed to be serial, it can be analyzed in terms of conventional chemical absorption theories. When the process is assumed to be in parallel, on the other hand, the absorption rate is influenced by coexistence of solid dissolution. That is, the dissolution of solids which can suspend in the liquid film enhances the absorption rate; the rate of solid dissolution is enhanced by the reaction between the dissolved gas and the dissolved solid in the liquid film.

The reaction in flue gas desulfurization using a slurry is regarded as being both consecutive and parallel. Evaluation of the desulfurization rate or the efficiency is further complicated by the coexistence of the solid dissolution. For example, the chemical reactions accompanying SO_2 absorption into $Mg(OH)_2$ slurry are considered to be

$$SO_2 + SO_3^{2-} + H_2O \rightarrow 2HSO_3^- \qquad (i)$$

and

0001-1541-83-6426-0060-$2.00.

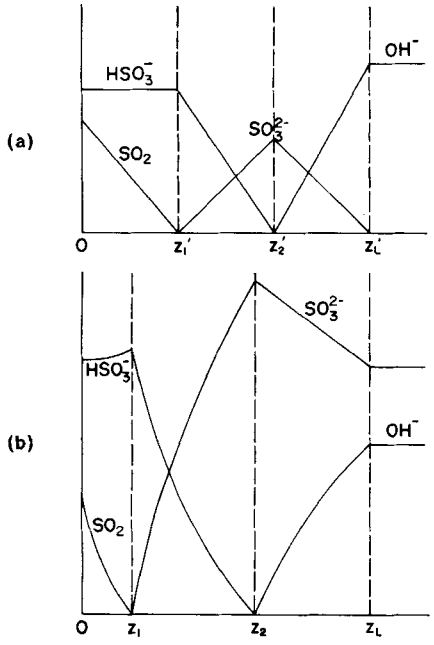

Figure 1. Conceptual concentration profiles in the desulfurization by magnesium hydroxide slurry.

$$HSO_3^- + OH^- \rightarrow SO_3^{2-} + H_2O, \qquad \text{(ii)}$$

and the chemical absorption process can be represented by a two-reaction plane model in which at one reaction plane, reaction (i) takes place and at another reaction plane, reaction (ii) takes place. For a clear solution saturated with $Mg(OH)_2$, a plausible sketch of the concentration profiles is given in Figure 1a. When fine $Mg(OH)_2$ particles are suspended in the liquid film, the concentration profiles will shift as shown in Figure 1b.

Also, the reaction sequence in desulfurization by $MgSO_4$-promoted limestone slurry starts with both the ion pair $MgSO_3^0$ (Cronkright and Leddy, 1976) and SO_3^{2-} as

$$SO_2 + MgSO_3^0 + H_2O \rightarrow Mg^{2+} + 2HSO_3^- \qquad \text{(iii)}$$

and reaction (i). As $CaCO_3$ is present, $MgSO_3^0$ and SO_3^{2-} are regenerated as

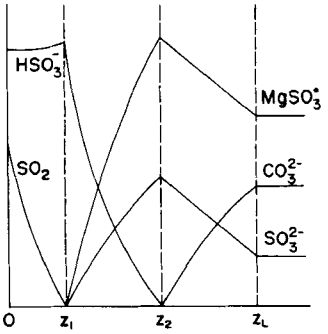

Figure 2. Conceptual concentration profiles in the desulfurization by magnesium sulfate-promoted limestone slurry.

$$Mg^{2+} + 2HSO_3^- + CO_3^{2-} \rightarrow MgSO_3^0 + SO_3^{2-} + CO_2 + H_2O. \qquad \text{(iv)}$$

The desulfurization process can be represented by the two-reaction-plane model where at one reaction plane, reactions (i) and (iii) take place and at another reaction plane, reaction (iv) takes place as conceptually sketched in Figure 2. The rate of solid dissolution in the liquid film is promoted by reaction (iv) when the particle size is considerably smaller than the thickness of liquid film.

In the previous papers (Sada et al., 1981a and 1981b), the above desulfurization processes were analyzed in terms of the two-reaction plane model incorporating solid dissolution enhanced by the reaction with dissolved SO_2 in the liquid film. Also, theoretical enhancement factors compared considerably well with the experimental data using a stirred tank absorber with a plane gas-liquid interface.

In the case of simple limestone, a major drawback is the poor mass transfer rate. It has been reported that addition of magnesium increases an effective sulfite concentration in the scrubbing liquor and this improves SO_2 removal (Cronkright and Leddy, 1976; Rochelle and King, 1977; Raymond and Sliger, 1978; Weismantel, 1978). However, little work has been done on the chemical absorption mechanism. In the present work, magnesium hydroxide was added to limestone slurry as a magnesium source. The desulfurization process by such a magnesium-promoted limestone slurry was formulated by the two-reaction plane model. To check the validity of the proposed model, the absorption of dilute SO_2 into an aqueous double slurry containing $CaCO_3$ and $Mg(OH)_2$ was carried out using a stirred vessel with a plane gas-liquid interface.

CONCLUSIONS AND SIGNIFICANCE

Poor performance in flue gas desulfurization by limestone slurry, which is attributed to large resistances to solid dissolution as well as mass transfer in liquid film, can be improved by addition of magnesium to the slurry. The magnesium sulfite ion pair, $MgSO_3^0$, has been thought to be responsible for the improved absorption efficiency. Little work has been done on modeling of such desulfurization systems. Magnesium hydroxide is chosen as a magnesium source and experiments have been carried out on the absorption of dilute SO_2 into aqueous double slurries of $CaCO_3$ and $Mg(OH)_2$ using a stirred tank with a plane gas-liquid interface at 298 K and 0.1013 MPa. Experimental results showed that the magnesium sulfite ion pair is responsible for the increased absorption rates. The present desulfurization process was formulated on the basis of the two-reaction plane model, in which there are no particles suspended in-between the interface and the primary reaction plane. It is deduced from comparisons between experimental and theoretical enhancement factors that 40 to 60% of the absorbed sulfur dioxide is present as the $MgSO_3^0$ ion pair.

CHEMICAL ABSORPTION MECHANISM: REACTION-PLANE MODEL

The reaction sequence in the desulfurization by a double slurry containing $CaCO_3$ and $Mg(OH)_2$ starts with both SO_3^{2-} and ion pair $MgSO_3^0$ as reactions (i) and (iii), respectively. When $CaCO_3$ and $Mg(OH)_2$ are present, $MgSO_3^0$ and SO_3^{2-} can be regenerated according to reaction (iv) and

$$Mg^{2+} + 2HSO_3^- + OH^- \rightarrow MgSO_3^0 + SO_3^{2-} + 2H_2O. \qquad \text{(v)}$$

In the $MgSO_4$-promoted limestone slurry, regeneration of $MgSO_3^0$ and SO_3^{2-} is established through reaction (iv) alone (Cronkright and

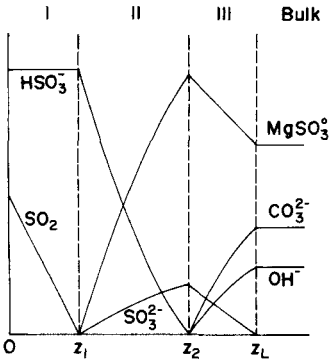

Figure 3. Conceptual concentration profiles of the relevant species in the desulfurization by limestone/magnesium hydroxide double slurry.

Leddy, 1976; Sada et al., 1981b).

Since reactions (i) through (v) are believed to be irreversible and instantaneous, there are two reaction planes forming in the liquid film. That is, at one reaction plane, the dissolved SO_2 reacts according to reactions (i) and (ii), and at another reaction plane, reactions (iv) and (v) take place to regenerate $MgSO_3^0$ and SO_3^{2-}.

Conceptual concentration profiles of the relevant species are sketched in Figure 3. When the average diameter of reactant particles is considerably smaller than the thickness of liquid film, the particles are suspended in the liquid film as well as in the bulk of liquid. It is, however, unrealistic to think that there may exist particles suspended in-between the gas-liquid interface and the primary reaction plane when the distance from the interface to the primary reaction plane is in the same order as or smaller than the mean diameter of particles as pointed out by Alper et al. (1980). To a first approximation, the sketch includes an assumption that there are no particles suspended in-between the interface and the primary reaction plane. Hence, the concentration profiles of species A (SO_2) and G (HSO_3^-) in region I are linear with the distance coordinate. The dissolution rates of $CaCO_3$ and $Mg(OH)_2$ particles in region II are promoted by reactions (iv) and (v), respectively. In region III, CO_3^{2-} (B_1) and OH^- (B_2) are fed through the physical dissolution of the particles. The concentration profiles of species E ($MgSO_3^0$) and F (SO_3^{2-}) are linear with distance because there is no reaction occurring near the suspended particles.

The film-theory conservation equations for the relevant species in regions I, II and III as shown in Figure 3 are written in dimensionless form as follows:

In region I,

$$\frac{d^2Y_A}{dx^2} = 0 \tag{1}$$

$$\frac{d^2Y_G}{dx^2} = 0 \tag{2}$$

In region II,

$$\frac{d^2Y_E}{dx^2} + \left(\frac{N_1 r_G}{2r_E} + \frac{N_2 r_G}{r_E}\right) Y_G = -\frac{N_1 + \alpha r_{B_2} N_2}{r_E} \tag{3}$$

$$\frac{d^2Y_F}{dx^2} + \frac{r_G}{r_F}\left(\frac{N_1}{2} + N_2\right) Y_G = -\frac{N_1 + \alpha r_{B_2} N_2}{r_F} \tag{4}$$

$$\frac{d^2Y_G}{dx^2} - (N_1 + N_2) Y_G = \frac{2N_1 + \alpha r_{B_2} N_2}{r_G} \tag{5}$$

In region III,

$$\frac{d^2Y_{B_1}}{dx^2} - N_1 Y_{B_1} = -N_1 \tag{6}$$

$$\frac{d^2Y_{B_2}}{dx^2} - N_2 Y_{B_2} = -\alpha N_2 \tag{7}$$

$$\frac{d^2Y_E}{dx^2} = 0 \tag{8}$$

$$\frac{d^2Y_F}{dx^2} = 0 \tag{9}$$

The boundary conditions are:

$$x = 0;\ Y_A = 1,\ dY_G/dx = 0 \tag{10}$$

$$x = x_1;\ Y_A = Y_E = Y_F = 0,\ Y_G = Y_G^* \tag{11}$$

$$-r_A q_A \frac{dY_A}{dx} = r_E \frac{dY_E}{dx} + r_F \frac{dY_F}{dx} \tag{12}$$

$$-r_G \frac{dY_G}{dx} = 2r_E \frac{dY_E}{dx} + 2r_F \frac{dY_F}{dx} \tag{13}$$

$$x = x_2;\ Y_{B_1} = Y_{B_2} = Y_G = 0,\ Y_E = Y_E^*,\ Y_F = Y_F^* \tag{14}$$

$$\left.\frac{dY_{B_1}}{dx}\right|_{x_2^+} + \frac{r_{B_2}}{2}\left.\frac{dY_{B_2}}{dx}\right|_{x_2^+} = -\frac{r_G}{2}\left.\frac{dY_G}{dx}\right|_{x_2^-} \tag{15}$$

$$= r_E \left.\frac{dY_E}{dx}\right|_{x_2^-} - r_E \left.\frac{dY_E}{dx}\right|_{x_2^+} \tag{16}$$

$$= r_F \left.\frac{dY_F}{dx}\right|_{x_2^-} - r_F \left.\frac{dY_F}{dx}\right|_{x_2^+} \tag{17}$$

$$x = 1;\ Y_{B_1} = 1,\ Y_{B_2} = \alpha,\ Y_E = Y_{E_0},\ Y_F = Y_{F_0}. \tag{18}$$

Here, Eqs. 12, 13 and 15–17 can be given from the stoichiometric balances at two reaction planes.

Solution of Eqs. 1 through 9 subject to Eqs. 10, 11 and 14–18 gives dimensionless concentrations as

In region I,

$$Y_A = 1 - \frac{x}{x_1} \tag{19}$$

$$Y_G = Y_G^* \tag{20}$$

In region II,

$$Y_{E,F} = -\left(\frac{r_G}{2r_{E,F}}\right)\left(\frac{N_1 + 2N_2}{N_1 + N_2}\right)\left[Y_G^* + \frac{2N_1 + \alpha r_{B_2} N_2}{r_G(N_1 + N_2)}\right] \times \frac{\sinh\sqrt{N_1 + N_2}(x_2 - x)}{\sinh\sqrt{N_1 + N_2}(x_2 - x_1)} - \left(\frac{1}{2r_{E,F}}\right) \times \frac{(2N_1 + \alpha r_{B_2} N_2)(N_1 + 2N_2)}{(N_1 + N_2)^2} \frac{\sinh\sqrt{N_1 + N_2}(x - x_1)}{\sinh\sqrt{N_1 + N_2}(x_2 - x_1)} - \left[\left(\frac{r_G}{2r_{E,F}}\right)\left(\frac{N_1 + 2N_2}{N_1 + N_2}\right) Y_G^* - Y_{E,F}^*\right] \frac{x}{x_2 - x_1} + \left(\frac{1}{2r_{E,F}}\right) \times \left(\frac{N_1 + 2N_2}{N_1 + N_2}\right)\left(\frac{r_G Y_G^* x_2}{x_2 - x_1} + \frac{2N_1 + \alpha r_{B_2} N_2}{N_1 + N_2}\right) - \frac{Y_{E,F}^* x_1}{x_2 - x_1} \tag{21, 22}$$

$$Y_G = \left[Y_G^* + \frac{2N_1 + \alpha r_{B_2} N_2}{r_G(N_1 + N_2)}\right] \frac{\sinh\sqrt{N_1 + N_2}(x_2 - x)}{\sinh\sqrt{N_1 + N_2}(x_2 - x_1)} + \left[\frac{2N_1 + \alpha r_{B_2} N_2}{r_G(N_1 + N_2)}\right] \frac{\sinh\sqrt{N_1 + N_2}(x - x_1)}{\sinh\sqrt{N_1 + N_2}(x_2 - x_1)} - \frac{2N_1 + \alpha r_{B_2} N_2}{r_G(N_1 + N_2)} \tag{23}$$

In region III,

$$Y_{B_1} = 1 - \frac{\sinh\sqrt{N_1}(1 - x)}{\sinh\sqrt{N_1}(1 - x_2)} \tag{24}$$

$$Y_{B_2} = \alpha - \frac{\alpha \sinh\sqrt{N_2}(1 - x)}{\sinh\sqrt{N_2}(1 - x_2)} \tag{25}$$

$$Y_{E,F} = -\frac{Y_{E,F}^* - Y_{E_0,F_0}}{1 - x_2} + \frac{Y_{E,F}^* - Y_{E_0,F_0} x_2}{1 - x_2} \tag{26, 27}$$

where Y_E^*, Y_F^* and Y_G^* are given by

$$Y_{E,F}^* = \frac{(x_2 - x_1)(1 - x_2)}{r_E(1 + x_2 - 2x_1)} \times \left[-\frac{\{r_G Y_G^* + (2N_1 + \alpha r_{B_2} N_2)/(N_1 + N_2)\} N_2}{\sqrt{N_1 + N_2}\sinh\sqrt{N_1 + N_2}(x_2 - x_1)} + \frac{(2N_1 + \alpha r_{B_2} N_2) N_2 \sqrt{N_1 + N_2}}{(N_1 + N_2)^2 \tanh\sqrt{N_1 + N_2}(x_2 - x_1)} + \frac{r_G(N_1 + 2N_2) Y_G^*}{(x_2 - x_1)(N_1 + N_2)} + \frac{2r_{E,F} Y_{E_0,F_0}}{1 - x_2}\right] \tag{28, 29}$$

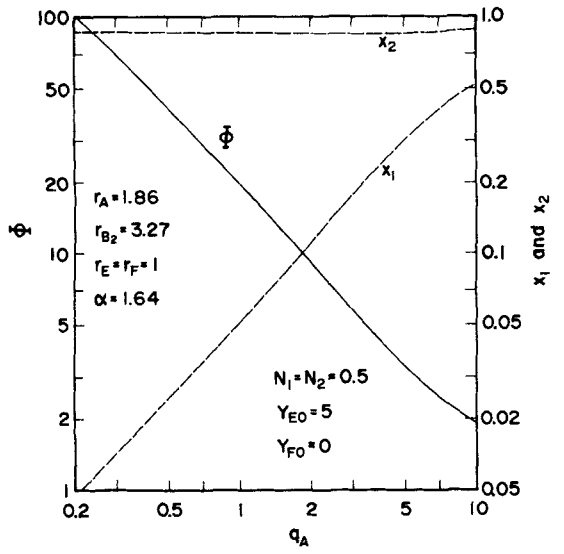

Figure 4. An example of enhancement factor and dimensionless positions of two reaction planes.

$$Y_G^* = \frac{\sinh\sqrt{N_1+N_2}(x_2-x_1)}{r_G\sqrt{N_1+N_2}}\left[\frac{2\sqrt{N_1}}{\tanh\sqrt{N_1}(1-x_2)} + \frac{\alpha r_{B_2}\sqrt{N_2}}{\tanh\sqrt{N_2}(1-x_2)} + \left(\frac{2N_1+\alpha r_{B_2}N_2}{N_1+N_2}\right) \times \frac{\sqrt{N_1+N_2}}{\tanh\sqrt{N_1+N_2}(x_2-x_1)}\right] - \frac{2N_1+\alpha r_{B_2}N_2}{r_G(N_1+N_2)}. \quad (30)$$

The dimensionless positions of two reaction planes, x_1 and x_2, can be determined by the following relations which are derived from the boundary conditions 12 and 13, respectively.

$$\frac{r_A q_A}{x_1} - \left(\frac{N_1+2N_2}{N_1+N_2}\right)\left(r_G Y_G^* + \frac{2N_1+\alpha r_{B_2}N_2}{N_1+N_2}\right) \times \frac{\sqrt{N_1+N_2}}{\tanh\sqrt{N_1+N_2}(x_2-x_1)} + \frac{(2N_1+\alpha r_{B_2}N_2)(N_1+2N_2)}{(N_1+N_2)^2} \times \frac{\sqrt{N_1+N_2}}{\sinh\sqrt{N_1+N_2}(x_2-x_1)} + \frac{r_G\{(N_1+2N_2)/(N_1+N_2)\}Y_G^* - r_E Y_E^* - r_F Y_F^*}{x_2-x_1} = 0 \quad (31)$$

$$\left\{2\left(\frac{N_1+2N_2}{N_1+N_2}\right)-1\right\}\left(r_G Y_G^* + \frac{2N_1+\alpha r_{B_2}N_2}{N_1+N_2}\right) \times \frac{\sqrt{N_1+N_2}}{\tanh\sqrt{N_1+N_2}(x_2-x_1)} - \left\{2\left(\frac{N_1+2N_2}{N_1+N_2}\right)-1\right\} \times \left(\frac{2N_1+\alpha r_{B_2}N_2}{N_1+N_2}\right)\frac{\sqrt{N_1+N_2}}{\sinh\sqrt{N_1+N_2}(x_2-x_1)} - \frac{2[r_G\{(N_1+2N_2)/(N_1+N_2)\}Y_G^* - r_E Y_E^* - r_F Y_F^*]}{x_2-x_1} = 0 \quad (32)$$

The enhancement factor is given as

$$\Phi = -\left.\frac{dY_A}{dx}\right|_{x=0} = \frac{1}{x_1}. \quad (33)$$

Figure 4 shows a typical example of computed results where the enhancement factor and the dimensionless positions of two reaction planes are plotted against q_A.

EXPERIMENTAL

Experiments were performed on the absorption of dilute SO_2 into aqueous double slurries of $CaCO_3$ and $Mg(OH)_2$ at 298 K and 0.1013 MPa. Also, some experiments were performed on the absorption into aqueous $MgSO_3$ slurries at the same conditions. The absorber used was a stirred tank with a plane gas-liquid interface, which was the same one as in our previous work (i.d. 100 mm and liquid volume 750 cm^3) (Sada et al., 1981b). It was operated batchwise in the liquid phase and continuously in the gas phase. The liquid and gas phase were agitated by separate motors at constant speeds of 180 and 800 rpm, respectively. The solute gas SO_2 was supplied from a cylinder of 4.73% concentration balanced by N_2, and further diluted with N_2 to the desired concentration before being fed to the absorber. The concentration of SO_2 in the influent and effluent streams were determined by UV derivative spectrophotometry (YANACO UO-1 derivative spectrophotometer). The absorption rate was calculated from the difference between the influent and effluent gas phase concentrations and the total gas flow rate.

EXPERIMENTAL RESULTS AND DISCUSSION

Experimental results on the absorption of SO_2 into aqueous double slurries of $CaCO_3$ and $Mg(OH)_2$ are shown in Figures 5a and 5b. The concentrations of $CaCO_3$ and $Mg(OH)_2$ in aqueous slurries were varied from 1 to 3 wt. % and 0.25 to 1 wt. %, respectively. The absorption rate N_A increased and accordingly, the corresponding gas phase concentration decreased with time, and finally reached that under the completely gas-film controlled conditions, N_A^∞. Both figures show the variation of N_A/N_A^∞ with process time. It is apparent from these figures that the absorption rate is increased by addition of $Mg(OH)_2$ and by adding 1 wt. % of $Mg(OH)_2$ to the $CaCO_3$ slurry, the rate of absorption into 2 wt. %-$CaCO_3$ slurry almost agrees with that into 3 wt. %-$CaCO_3$ slurry. In Figure 6, the variation of the absorption rate with process time was indicated as a relation of N_A to y_{Ao} which is an implicit function of time. The plot is independent of the slurry concentration because the SO_2 concentration in the influent stream and the total gas flow rate are both constant at 1775 ppm and 23.7 cm^3/s, respectively. That is, the relationship between N_A and y_{Ao} is uniquely given as

$$y_{Ao} = y_{Af} - \frac{10^6 A_t}{V_t} N_A. \quad (34)$$

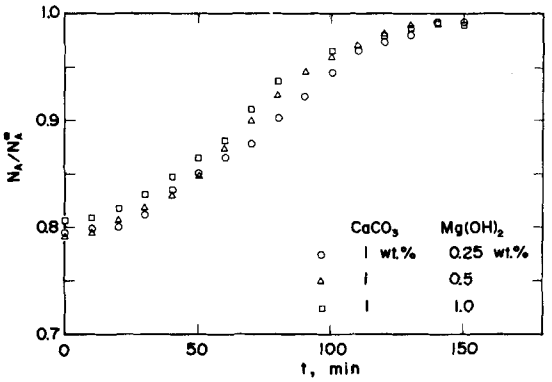

Figure 5a. Variation of relative absorption rate with process time for 1 wt. % $CaCO_3$ slurry.

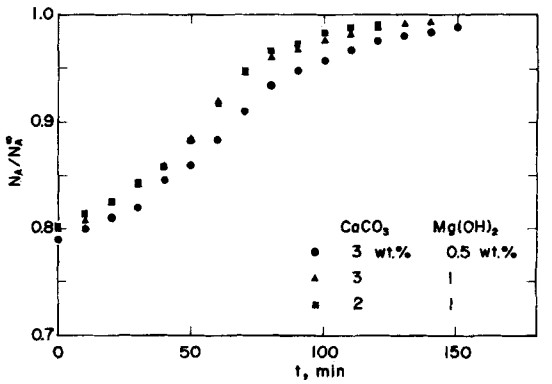

Figure 5b. Variation of relative absorption rate with process time.

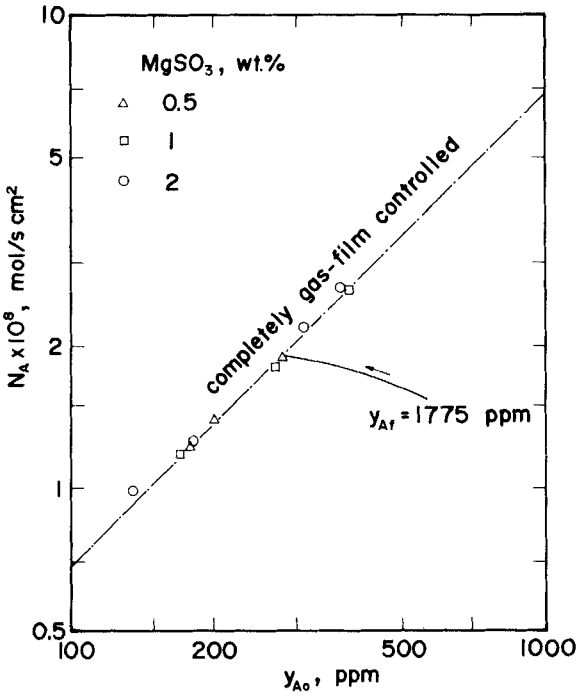

Figure 6. Variation of SO_2 absorption rate with time for the absorption into the double slurry and observed SO_2 absorption rates into aqueous slurries of only $MgSO_3$ as a function of y_{Ao}.

In the same figure, the absorption rate into aqueous slurries of only $MgSO_3$ was also plotted against the gas-phase concentration. In fact, the rate of absorption into the $MgSO_3$ slurries essentially remained constant with respect to the process time, and agreed with that under the completely gas-film controlled conditions.

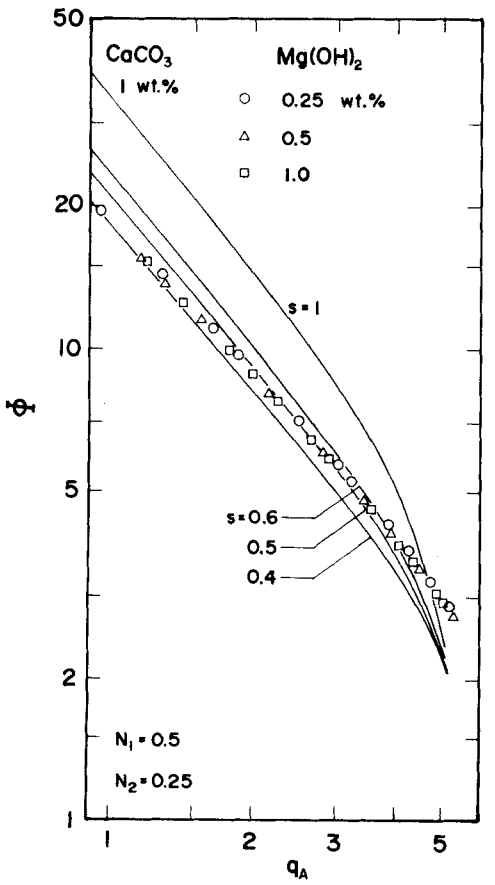

Figure 7a. Variation of enhancement factor with time and comparison with theoretical enhancement factor for 1 wt. % $CaCO_3$ slurry.

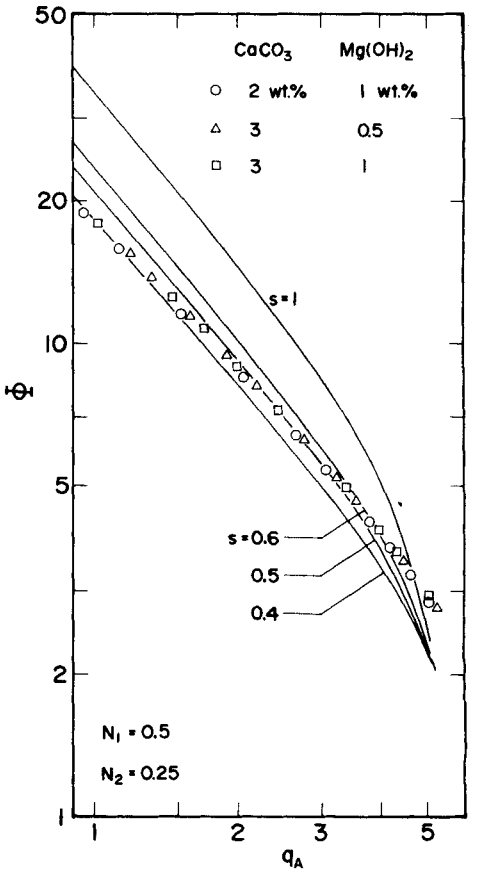

Figure 7b. Variation of enhancement factor with time and comparison with theoretical enhancement factor.

Some fraction of the sulfur dioxide absorbed in the double slurry is accumulated as $MgSO_3^0$ ion pair as would be expected and it is considered that the accumulated ion pair is responsible for the increased absorption rate. The variation of the enhancement factor with process time was indicated in Figures 7a and 7b as a plot of Φ vs. q_A. Here, it should be noted that q_A is an implicit function of time and Φ is independent of the slurry concentration. The full curves represent the theoretical enhancement factors according to the two-reaction-plane model described in the previous section, in which the concentration of $MgSO_3^0$ ion pair in the bulk liquid phase at any time is calculated from the total amount of the sulfur dioxide absorbed by that time. The parameters N_1 and N_2 were fixed at 0.5 and 0.25, which approximately correspond to the 2 wt. %- and 1 wt. %-slurry, respectively (Sada et al., 1981a). Both parameters, however, have little influence on the absorption rate or the enhancement factor. The parameter s denotes the ratio of the concentration of $MgSO_3^0$ ion pair in the bulk liquid phase to the total concentration of sulfur dioxide absorbed. For example, $s = 0.4$ means that 40 percent of the absorbed sulfur dioxide by any time is present as $MgSO_3^0$ ion pair. It is deduced from both figures that 40 to 60 percent of the absorbed sulfur dioxide will be present as $MgSO_3^0$ ion pair. This is equivalent to the fact that the $MgSO_3^0$ ion pair and the SO_3^{2-} species are regenerated almost equimolecularly by reactions (iv) and (v).

Experimental results here suggest that in practical situations where slurry is recirculated, dissolved sulfur dioxide reacts mainly with the $MgSO_3^0$ ion pair and the absorption rate is completely controlled by the gas-film resistance.

NOTATION

A_{pl} = surface area of $CaCO_3$ particles, cm^2/cm^3-dispersion

A_{p2} = surface area of $Mg(OH)_2$ particles, cm^2/cm^3-dispersion
A_t = total gas-liquid interfacial area, cm^2
C = concentration in liquid phase, mol/cm^3
D = diffusivity in liquid phase, cm^2/s
k_{s1} = mass transfer coefficient for $CaCO_3$ particle dissolution, cm/s
k_{s2} = mass transfer coefficient for $Mg(OH)_2$ particle dissolution, cm/s
N_1 = $k_{s1}A_{p1}z_L^2/D_{B1}$
N_2 = $k_{s2}A_{p2}z_L^2/D_{B2}$
N_A = absorption rate of SO_2, $mol/s\cdot cm^2$
N_A^∞ = absorption rate of SO_2 under completely gas-film controlled conditions, $mol/s\cdot cm^2$
q_A = dimensionless interfacial concentration of $A = C_{Ai}/C_{B1s}$
r_I = ratio of diffusivity of species I to that of species $B_1 = D_I/D_{B1}$
s = ratio of $MgSO_3^0$ ion pair concentration formed in bulk liquid phase to total SO_2 concentration absorbed
V_t = total gas flow rate, mol/s
x = dimensionless distance = z/z_L
x_1 = dimensionless position of primary reaction plane = z_1/z_L
x_2 = dimensionless position of secondary reaction plane = z_2/z_L
Y_A = dimensionless concentration of A in liquid phase relative to that at gas-liquid interface = C_A/C_{Ai}
Y_I = dimensionless concentration of species I (= B_2, E, F and G) in liquid phase relative to that of B_1 at $CaCO_3$ particle surface = C_I/C_{B1}
y_A = concentration of SO_2 in gas phase, ppm
z = distance into liquid phase from gas-liquid interface, cm
z_1 = position of primary reaction plane, cm
z_2 = position of secondary reaction plane, cm
z_L = thickness of liquid film (for gas absorption), cm
α = C_{B2}/C_{B1}
Φ = enhancement factor

Subscripts

A = dissolved gas (SO_2)
B_1 = CO_3^{2-}
B_2 = OH^-
E = $MgSO_3^0$
F = SO_3^{2-}
f = influent stream
G = HSO_3^-
i = gas-liquid interface
o = effluent stream
s = solid surface
0 = bulk of liquid

Superscript

* = value at primary or secondary reaction plane

LITERATURE CITED

Alper, E., B. Wichtendahl, and W.-D. Deckwer, "Gas Absorption Mechanism in Catalytic Slurry Reactors," *Chem. Eng. Sci.*, **35**, 217 (1980).

Cronkright, W. A., and W. J. Leddy, "Improving Mass Transfer Characteristics of Limestone Slurries by Use of Magnesium Sulfate," *Env. Sci. Tech.*, **10**, 569 (1976).

Raymond, W. J., and A. G. Sliger, "The Kellogg/Weir Scrubbing System," *Chem. Eng. Prog.*, 75 (Feb., 1978).

Rochelle, G. T., and C. J. King, "The Effect of Additives on Mass Transfer in $CaCO_3$ or CaO Slurry Scrubbing of SO_2 from Waste Gases," *Ind. Eng. Chem. Fund.*, **16**, 67 (1977).

Sada, E., H. Kumazawa, Y. Sawada, and I. Hashizume, "Kinetics of Absorptions of Lean Sulfur Dioxide into Aqueous Slurries of Calcium Carbonate and Magnesium Hydroxide," *Chem. Eng. Sci.*, **36**, 149 (1981a).

Sada, E., H. Kumazawa, I. Hashizume, and N. Kamishima, "Desulfurization by Limestone Slurry with Added Magnesium Sulfate," *Chem. Eng. J.*, **22**, 133 (1981b).

Weismantel, G. E., "Limestone + Magnesium: A New SO_2 Control Team," *Chem. Eng.*, 111 (Sept. 11, 1978).

Manuscript received September 14, 1981; revision received December 16, and accepted January 13, 1982.